RelA/p65 promotes osteoclast differentiation by blocking a RANKL-induced apoptotic JNK pathway in mice

Sergio Vaira,[1] Muhammad Alhawagri,[1] Imani Anwisye,[1] Hideki Kitaura,[2] Roberta Faccio,[2] and Deborah Veis Novack[1,3]

[1]Division of Bone and Mineral Diseases, Department of Medicine, [2]Department of Orthopedic Surgery, and [3]Department of Pathology, Washington University School of Medicine, St. Louis, Missouri, USA.

Osteoclasts (OCs) function to reabsorb bone and are responsible for the bone loss associated with inflammatory arthritis and osteoporosis. OC numbers are elevated in most disorders of accelerated bone destruction, reflecting altered rates of precursor differentiation and apoptosis. Both of these processes are regulated by the JNK family of MAP kinases. In this study, we have demonstrated that the NF-κB subunit RelA/p65 inhibits JNK-mediated apoptosis during a critical period of commitment to the OC phenotype in response to the cytokine RANKL. This RelA/p65-mediated arrest of cell death led to enhanced OC differentiation. Hence, *Rela*−/− OC precursors displayed prolonged JNK activation in response to RANKL, and this was accompanied by an increase in cell death that prevented efficient differentiation. Although complete blockade of JNK activity inhibits osteoclastogenesis, both short-term blockade in RelA-deficient cultures and suppression of the downstream mediator, Bid rescued apoptosis and differentiation. These antiapoptotic effects were RelA specific, as overexpression of RelA, but not RelB, blocked apoptosis and rescued differentiation in *Rela*−/− precursors. Thus, RelA blocks a RANKL-induced, apoptotic JNK-Bid pathway, thereby promoting OC differentiation. Consistent with this, mice lacking RelA/p65 in the hematopoietic compartment were shown to have a deficient osteoclastogenic response to RANKL and were protected from arthritis-induced osteolysis.

Introduction

Osteoclasts (OCs) are multinucleated cells derived from myeloid bone marrow progenitors that express RANK, the receptor for the key osteoclastogenic cytokine RANKL (1). Increased OC formation and activity is observed in many osteopenic disorders, including postmenopausal osteoporosis, lytic bone metastasis, and rheumatoid arthritis, and leads to pain and structural instability. Osteoblast lineage cells express a membrane-bound form of RANKL, a member of the TNF cytokine family. Like other members of the TNF receptor superfamily, RANK strongly activates the NF-κB pathway.

In mammals, the NF-κB family has 5 members: RelA/p65, RelB, c-Rel, NF-κB1/p50, and NF-κB2/p52 (2). In the canonical NF-κB pathway, ligation of RANK activates the inhibitor of IκB kinase (IKK) complex, which phosphorylates NF-κB–associated IκBα, leading to its ubiquitination and proteosomal degradation. These events release NF-κB dimers containing RelA and c-Rel in the cytosol, allowing them to translocate into the nucleus where they enhance transcription of target genes. In the alternative NF-κB pathway, NF-κB–inducing kinase (NIK) and IKKα target p100 for ubiquitination and processing, thereby allowing nuclear translocation of predominantly RelB-containing dimers.

The importance of NF-κB in osteoclastogenesis has been highlighted by several mouse models. Mice lacking both NF-κB1 and NF-κB2 have severe osteopetrosis with complete absence of OCs

(3, 4). Ablation of IKKβ, a key component of the IKK complex, blocks nuclear translocation of RelA, RelB, and c-Rel and leads to increased bone mass and OC lineage apoptosis (5). Transduction of OC precursors with a superrepressor of IκBα that cannot be proteasomally degraded blocks OC differentiation and survival (6, 7). Additionally, we have previously shown that ablation of NIK inhibits both RelA and RelB nuclear translocation in pre-OCs, leading to a resistance to RANKL-induced osteoclastogenesis in vivo and in vitro (8). Consistent with this observation, osteoclastogenesis and hence bone erosion are reduced in the serum transfer model of inflammatory arthritis in *Nik*−/− mice (9). These data suggest that tight regulation of the classical and alternative pathways is critical to the OC in both physiological and pathological circumstances. However, none of the previous studies have addressed the role of individual subunits in the OC response to RANKL.
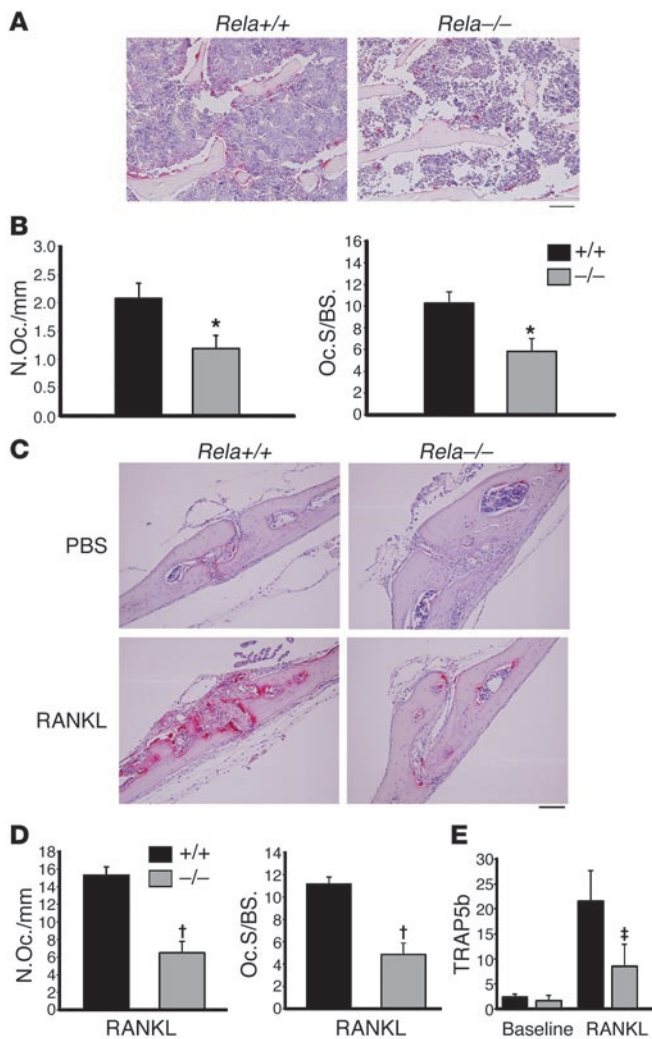
Ablation of RelA in mice causes embryonic lethality, with extensive liver apoptosis at E15.5 (10), dependent on TNF-α. Thus, deficiency of either p55 TNF receptor (TNFR1) or TNF-α rescues this hepatic event and allows the doubly mutant mice to live at least to postnatal day 14–21 (11, 12). Ablation of TNFR1 in the IKKβ mutant mice also restored OC numbers in vivo, suggesting that TNF is the main driver of apoptosis in this lineage as well (5). One report has suggested that RANKL also induces OC lineage apoptosis, despite the lack of a death domain in its receptor RANK (13), although the mechanism has not been extensively explored.

Using genetic knockout approaches, the specific role of RelA has previously been examined in lymphocytes, lymph node stroma, hepatocytes, and neurons. Although several groups have demonstrated potent RelA activation in OCs in response to RANKL and/or TNF, no studies have specifically addressed the unique role of this subunit. We have now used *Rela*−/−*Tnfr1*−/− mice to explore the role

Figure 1
RelA is important for basal and stimulated OC formation in vivo. (**A**) TRAP-stained sections of vertebrae from *Rela*^{+/+} and *Rela*^{–/–} RCs 4 months after bone marrow reconstitution. Scale bar: 100 μm. (**B**) Histomorphometric analysis was performed on TRAP-stained sections to determine the OC number (N.Oc./mm) and OC surface (Oc.S./BS.). *$P < 0.05$; $n = 8$/group. (**C**) *Rela*^{+/+} and *Rela*^{–/–} RCs were injected with 100-μg RANKL or PBS daily for 5 days and sacrificed on the sixth day. TRAP-stained coronal sections of calvaria at the sagittal suture show a consistent increase in OCs along sutures and sinusoids only in *Rela*^{+/+} RANKL-treated animals. Scale bar: 200 μm. (**D**) Quantification of the N.Oc./mm and Oc.S./BS. (percentage of bone surface covered by OCs) along calvarial surfaces of mice in **C** confirms the significant difference in response of *Rela*^{+/+} and *Rela*^{–/–} RCs to RANKL injection. In the PBS-injected animals, only rare OCs are detected in either genotype. †$P < 0.005$; $n = 5$/group. (**E**) Serum levels of TRAP5b were determined 1 day prior to first RANKL injection (baseline) and at sacrifice on day 6 (RANKL). ‡$P = 0.01$; $n = 5$/group.

The key cytokine required for OC differentiation from monocyte lineage precursors is RANKL. To examine the osteoclastogenic response to RANKL more directly, we injected RANKL (100 μg/d, for 5 days subcutaneously) into *Rela*^{+/+} and *Rela*^{–/–} RCs. Examination of tartrate resistant acid phosphatase–stained (TRAP) calvaria sections showed that the *Rela*^{+/+} controls had an increased OC number along calvarial sinuses and sutures compared with the PBS-injected controls (Figure 1, C and D). In contrast, *Rela*^{–/–} RCs exhibited a blunted response to RANKL, indicated by fewer TRAP[+] OCs on histomorphometric analysis and a significantly smaller rise in serum TRAP5b levels (Figure 1E). Thus, RelA is important for RANKL-stimulated osteoclastogenesis in vivo.

Absence of RelA protects mice from arthritis-induced bone loss but not inflammation. Blockade of NF-κB reduces both inflammation and bone loss in several murine models of inflammatory arthritis (9, 14, 15). The *Rela*^{+/+} and *Rela*^{–/–} RCs were injected with K/BxN serum (16) on days 0, 2, and 7, with LPS on day 2, to induce serum transfer arthritis. Histological sections of hind paws harvested at day 14 were stained with H&E and TRAP. H&E sections from *Rela*^{+/+} and *Rela*^{–/–} RCs exhibited the same rate of infiltrate in the joint space, composed primarily of neutrophils (Figure 2A), and the thickness of the hind paws of *Rela*^{–/–} RCs was very similar to those of *Rela*^{+/+} controls through day 14 (Figure 2B), indicating that RelA is not important for the inflammatory response in this model. Another common feature of serum transfer arthritis is erosion of bones in the hind paw, with a large induction of osteoclastogenesis. Hind paws from *Rela*^{–/–} RCs had fewer OCs compared with *Rela*^{+/+} RCs, both on the bone surface and in adjacent marrow, with 4-fold fewer OCs on the external bone surfaces (Figure 2, C and D). These results correlated with blunted induction of the serum marker collagen C-terminal telopeptide (CTX) at day 14 in *Rela*^{–/–} RCs relative to *Rela*^{+/+} (Figure 2E). These results suggest that the RelA subunit is required for the osteoclastogenic response to inflammation.

RelA is important for OC precursor survival but not differentiation. To better understand the mechanism by which RelA impacts the OC, we turned to in vitro culture. In the presence of M-CSF and RANKL or in coculture with wild-type osteoblasts, bone marrow macrophages (BMMs) from RelA-deficient mice formed fewer OCs (Figure 3, A and B). The effect is dependent on the loss of RelA and not TNFR1, since reexpression of the latter did not rescue the phenotype (data not shown). During culture, we noticed fewer cells in RelA-deficient wells treated with RANKL and M-CSF, but

of RelA in the OC lineage and find that this subunit plays a critical role in opposing cell death induced by RANKL during OC differentiation. This apoptotic pathway is mediated by JNK and cannot be blocked by activation of RelB.

Results

Rela is important for RANKL-stimulated osteoclastogenesis in vivo. Although RelA-deficiency does not cause embryonic lethality on the *Tnfr1*^{–/–} background, the double-knockout mice live an average of only 2–3 weeks. In order to analyze the subunit-specific role of RelA in the OCs of adult mice, we generated radiation chimeras (RCs), engrafting C57BL/6J mice with bone marrow cells from *Rela*^{–/–}*Tnfr1*^{–/–} donors or *Rela*^{+/+}*Tnfr1*^{–/–} controls. Hematopoietic cells in the RCs are all *Tnfr1*^{–/–} regardless of *Rela* genotype, and we will subsequently refer to these RCs as either *Rela*^{+/+} or *Rela*^{–/–}. We performed histomorphometric analysis on vertebrae from RCs 4 months after engraftment and found a 50% decrease in OC number and surface in *Rela*^{–/–} relative to WT (Figure 1, A and B). There was no difference in trabecular bone volume (BV/TV) in *Rela*^{+/+} and *Rela*^{–/–} chimeras. However, others have failed to detect differences in BV/TV in RCs bearing marrow with strong OC phenotypes such as *RANK*^{–/–} (J. Lorenzo, personal communication).
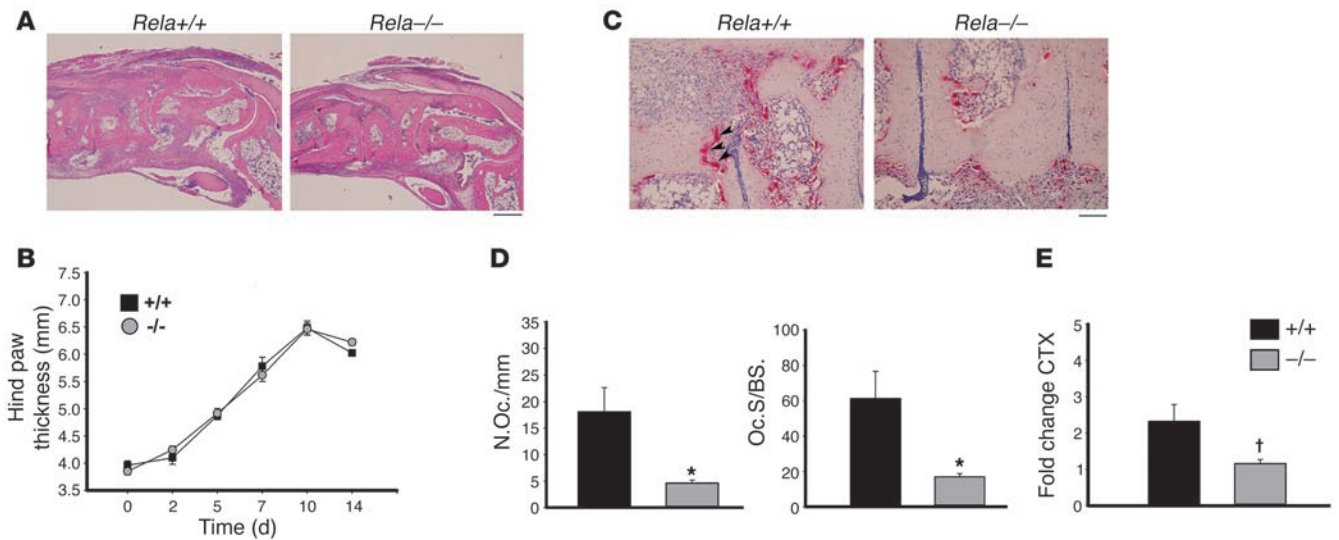
Figure 2
Rela⁻/⁻ RCs are protected from arthritis-induced bone loss. (**A**) Arthritis was induced in *Rela⁺/⁺* and *Rela⁻/⁻* RCs 5 weeks after marrow transplantation by injection of K/BxN serum at days 0, 2, and 7, with LPS on day 2. Histological sections of ankle joints at day 14 stained with H&E show an extensive and similar inflammatory infiltrate in the joint spaces. Scale bar: 500 μm. (**B**) The inflammatory response was also evaluated by measurement of hind paw thickness (sum of both paws) during induction of arthritis. *n* = 8/group. The experiment was repeated twice, with similar results. (**C**) TRAP-stained sections of metatarsals demonstrate OCs both on the outer bone surface adjacent to inflammatory pannus (arrowheads) and in marrow spaces. Scale bar: 100 μm. (**D**) Histomorphometric analysis of N.Oc./mm and Oc.S./BS. on the outer bone surface demonstrate significantly more OCs in *Rela⁺/⁺* RCs compared with *Rela⁻/⁻* RCs. *$P < 0.001$; *n* = 8/group. (**E**) Serum CTX was measured at day 0 and 14 of serum transfer arthritis, and the fold change for each RC was plotted, demonstrating a significant rise only in the *Rela⁺/⁺* group. †$P < 0.05$; *n* = 6/group.

not in RelA-deficient wells treated with M-CSF alone. MTT assays (3-4, 5-dimethylthiazol-2-y-2,5 diphenyltetrazolium bromide assays) confirmed a decreased cell number in *Rela⁻/⁻* cultures by 48 hours of RANKL treatment (Figure 3C), although there was no difference between *Rela⁺/⁺* and *Rela⁻/⁻* cells cultured in M-CSF alone (data not shown). These data suggested that RelA plays an antiapoptotic role. Therefore, we examined various markers of apoptosis in RANKL-stimulated cultures. In concordance with the MTT assay showing that significant cell loss in *Rela⁻/⁻* cultures occurs between 24 and 48 hours of RANKL treatment, a DNA fragmentation assay showed that *Rela⁻/⁻* cultures treated with RANKL for 36 hours, but not 18 hours, had 3- to 4-fold higher levels of DNA fragmentation than M-CSF treated controls (Figure 3D). Interestingly, *Rela⁺/⁺* cultures also had significant levels of DNA fragmentation after 36 hours of RANKL exposure, although the levels were much less than for similarly treated *Rela⁻/⁻*. This RANKL-mediated apoptosis, accentuated by the absence of RelA, was confirmed by examination of caspase-3. Using a fluorimetric assay (Figure 3E), we found that while caspase-3 activation increased modestly (2-fold) in *Rela⁺/⁺* precursors between 36 and 48 hours of RANKL exposure, caspase-3 was activated up to 4-fold in similarly treated *Rela⁻/⁻* cells during the same period. Caspase-9 activation was also elevated in the absence of RelA, while caspase-8 levels were unaffected (data not shown). These data indicate that RelA protects OC precursors from RANKL-induced cell death by blocking an intrinsic (caspase-3/9 dependent) apoptotic pathway during a critical period of differentiation (36–48 hours of RANKL exposure).

In order to determine if the failure to generate OCs was secondary to apoptosis and not due to a primary RelA effect on differentiation, we used the caspase inhibitor ZVAD, in conjunction with RANKL, during the first 48 hours of OC differentiation.

This treatment blocked the RANKL-induced caspase-3 activation (Figure 3E) and normalized the number of OCs generated from *Rela⁻/⁻* precursors after 6 days of culture (Figure 3F). We also found that *Rela⁻/⁻* OCs generated in the presence of ZVAD were able to form resorptive pits on bone slices (Figure 3G). These results demonstrate that RelA is important for OC precursor survival but not differentiation or function.

A JNK-Bid pathway causes RANKL-mediated apoptosis in the absence of RelA. NF-κB has been implicated in the control of many antiapoptotic genes, including *Bcl2*, *BclxL*, and the inhibitor of apoptosis (IAP) family (*Ciap1, -2, Xiap*). We therefore performed real-time quantitative PCR analysis to examine expression levels of these potential RelA targets in OC precursors. Of this group, only *xiap* was induced by RANKL in a RelA-dependent manner (Figure 4A, left panel). XIAP binds to and inhibits caspase-3 (17), and, therefore, may represent an important antiapoptotic signal controlled by RelA in response to RANKL in OC precursors.

In the context of TNF-α–mediated apoptosis, absence of RelA potentiates JNK activation. One mechanism is decreased via expression of Gadd45β, an inhibitor of the JNK kinase MKK7 (18). Others have described reduced activity of the MKP family of JNK phosphatases (19). In OC precursors, RANKL-induced expression of both *Gadd45b* and *Mkp5* in a RelA-dependent manner (Figure 4A), suggesting that JNK activation might also be altered in *Rela⁻/⁻* OC precursors. Although RANKL-induced JNK activation was normal in *Rela⁻/⁻* BMMs (data not shown), *Rela⁻/⁻* pre-OCs (BMMs cultured for 2 days in M-CSF and RANKL) showed stronger phosphorylation of JNK following starvation and restimulation with RANKL for 15 minutes (Figure 4B) and increased JNK kinase activity (data not shown). To determine whether this enhanced JNK activation is related to apoptosis in pre-OCs, we treated *Rela⁻/⁻* cultures
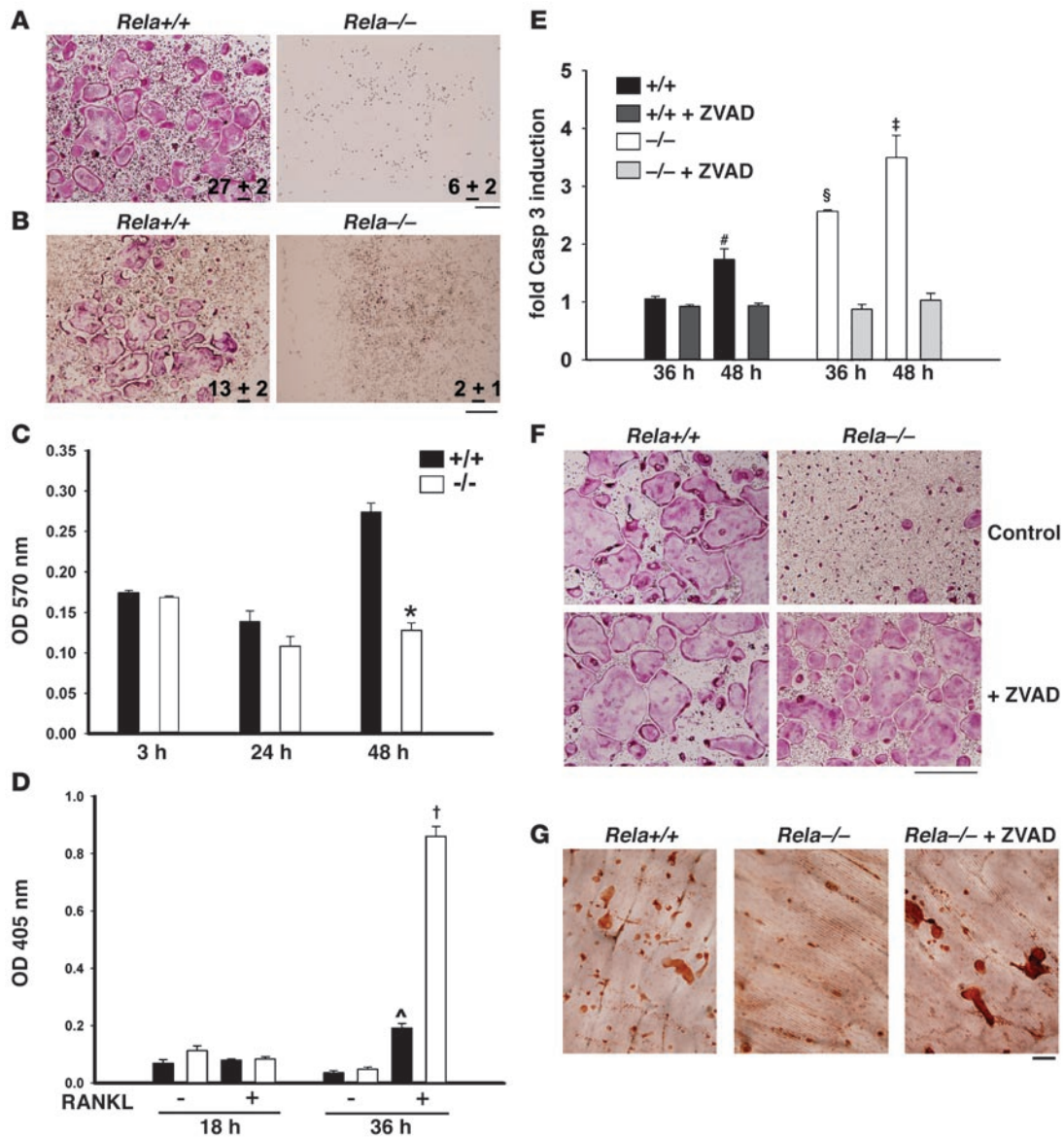
Figure 3

Rela^{−/−} BMMs are sensitive to RANKL-induced cell death. (**A**) *Rela*^{+/+} or *Rela*^{−/−} BMMs were cultured in M-CSF and RANKL or (**B**) cultured with wild-type calvarial osteoblasts in the presence of 1,25 vitamin D_3, then fixed and TRAP stained. Scale bar: 500 μm. The number of OCs per field (mean ± SEM) is shown, demonstrating fewer OCs in the absence of RelA. (**C**) Cell number was assessed by MTT assay in BMMs cultured with M-CSF and RANKL for 3–48 hours, showing fewer cells after 48 hours in *Rela*^{−/−} cultures relative to *Rela*^{+/+} (*P < 0.00001; n = 4). (**D**) Apoptosis was measured by DNA fragmentation assay after 18 or 36 hours in the presence of M-CSF, with (+) or without (−) RANKL. After 36 hours, *Rela*^{−/−} BMMs cultured with M-CSF and RANKL, but not with M-CSF alone, had increased cell death. ^P < 0.0001 compared with *Rela*^{+/+} without RANKL at 36 hours; †P < 0.00001 relative to *Rela*^{+/+} with RANKL at 36 hours. (**E**) Caspase-3 (casp 3) activation was measured in *Rela*^{+/+} and *Rela*^{−/−} BMMs cultured in M-CSF/RANKL for 36 and 48 hours, with or without ZVAD, and fold induction relative to the same cells in M-CSF alone was plotted. #P < 0.05 relative to *Rela*^{+/+} 36 hours; ‡P < 0.01, §P < 0.00001 relative to *Rela*^{+/+} at 36 or 48 hours. (**F**) OCs were generated with or without ZVAD during the first 48 hours. Scale bar: 500 μm. (**G**) OCs were generated as in **F** on cortical bone slices. Resorption pits (brown) were stained with horseradish peroxidase-conjugated wheat germ agglutinin. Scale bar: 100 μm.

with the JNK inhibitor SP600125, along with RANKL for 36 hours. Inhibition of JNK reduced DNA fragmentation to wild-type levels (Figure 4C) and restored osteoclastogenesis in *Rela*^{−/−} precursors (Figure 4D), suggesting that JNK is mechanistically involved in RANKL-induced apoptosis in RelA-deficient OC precursors.

Enhanced JNK activation appears to initiate apoptosis by activating Bid, a proapoptotic BH3-only member of Bcl-2 family, at least

in response to TNF (20). While Bid was expressed in both *Rela*^{+/+} and *Rela*^{−/−} BMM cultures, levels were not affected by RANKL treatment in either genotype (Figure 5A), and cleavage products were not detected. In order to determine whether Bid is responsible for RANKL-induced apoptosis, we employed a retroviral siRNA approach, using 2 different sequences to knock down Bid expression in *Rela*^{−/−} OC precursors. Levels of Bid in *Rela*^{−/−} BMMs
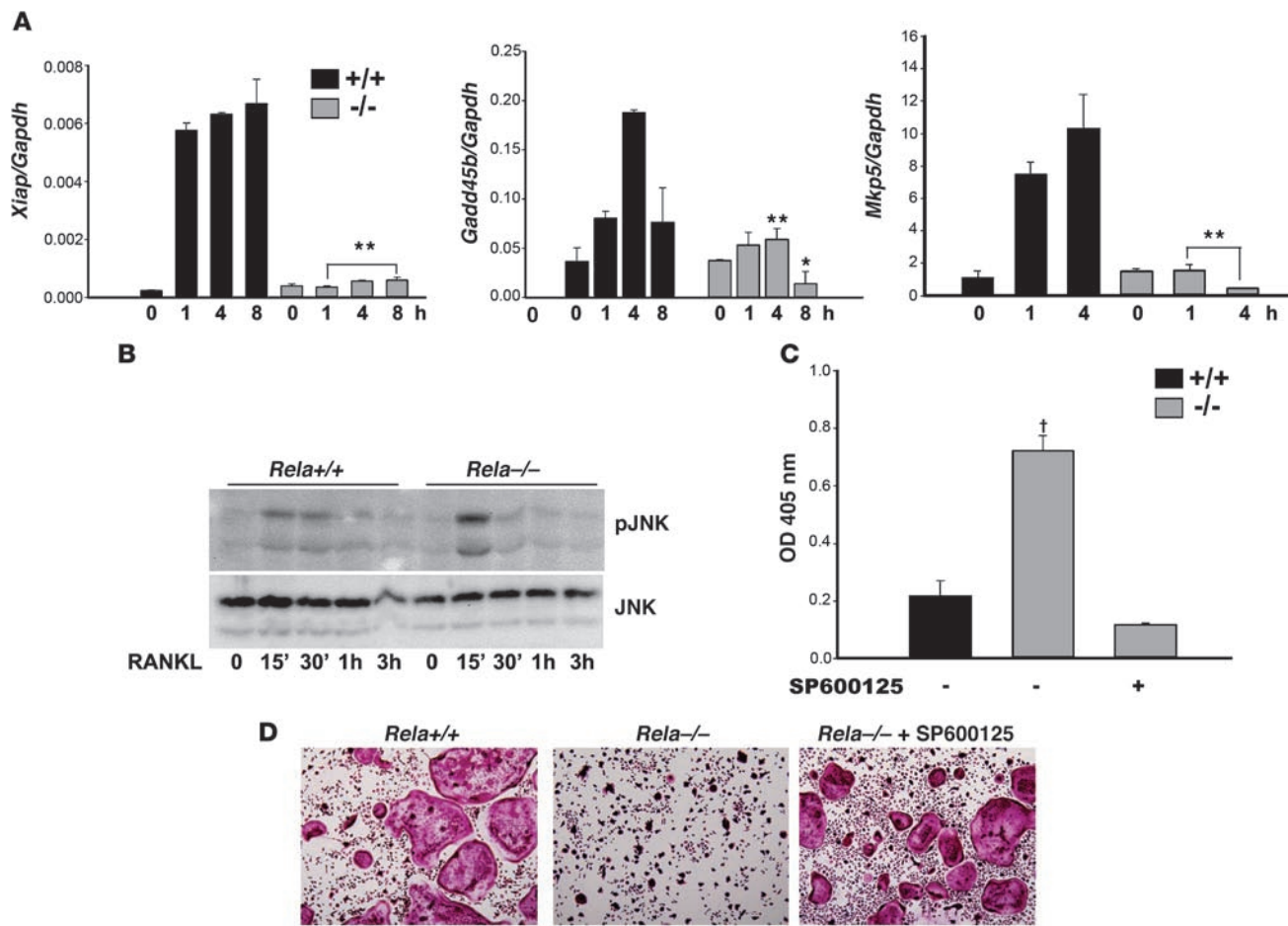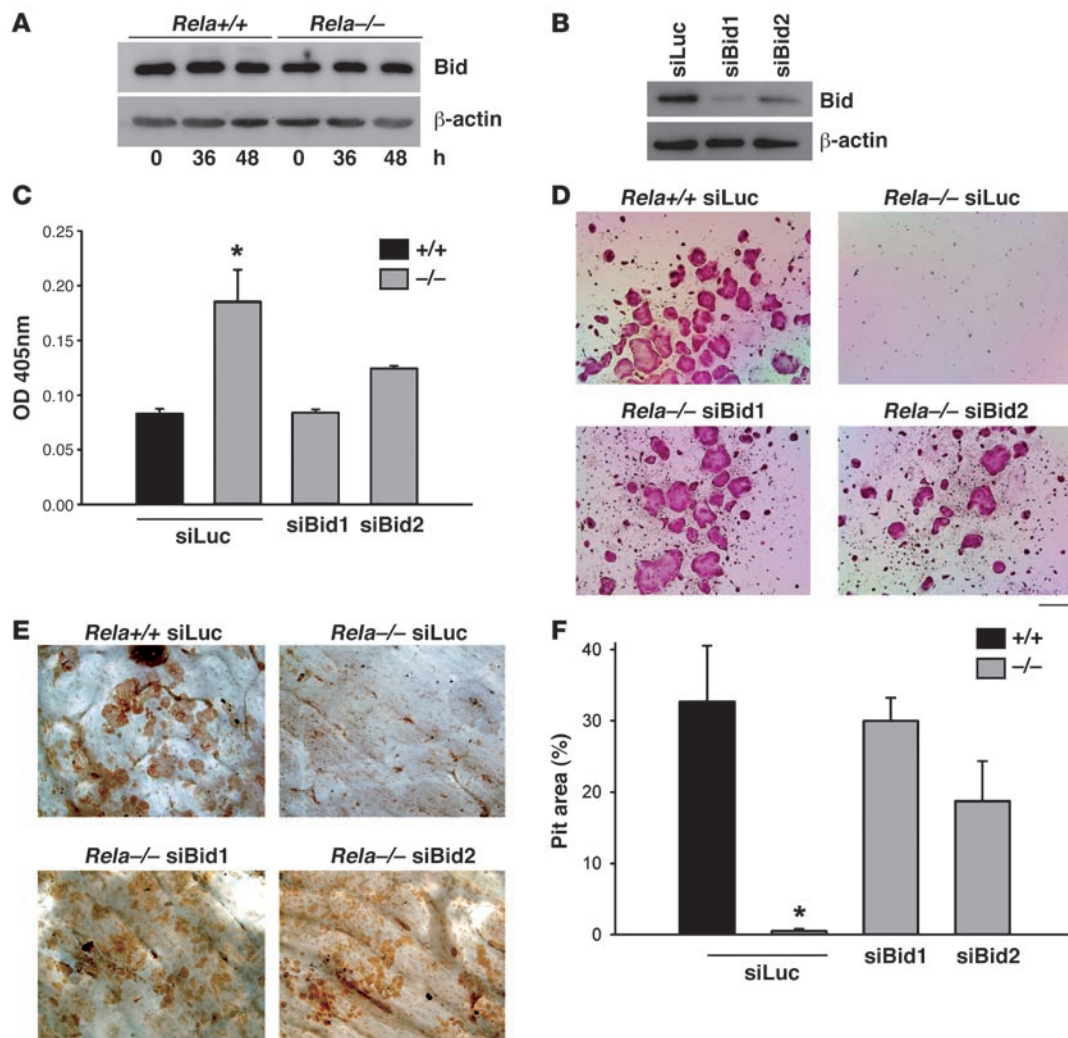
Figure 4

The absence of *RelA* leads to enhanced JNK activation. (**A**) Pre-OCs (BMMs cultured for 2 days with M-CSF and RANKL) generated from *Rela*^{+/+} (black bars) and *Rela*^{-/-} (gray bars) mice were then starved of serum and cytokines and restimulated with RANKL for the indicated times prior to RNA extraction and real-time quantitative PCR for *xiap*, *Gadd45b*, and *Mkp5*. *Rela*^{-/-} pre-OCs show significantly less induction of *xiap*, *Gadd45b* and *Mkp5*. *P < 0.5, **P < 0.01 compared to *Rela*^{+/+} at the same time point. (**B**) *Rela*^{+/+} and *Rela*^{-/-} pre-OCs were starved and restimulated with RANKL for the indicated times, and total lysates were analyzed by immunoblot for pJNK, demonstrating enhanced JNK activation in *Rela*^{-/-} cultures. A parallel blot with equal loading was used to assess total JNK protein. (**C**) *Rela*^{+/+} and *Rela*^{-/-} BMMs were cultured in RANKL, with or without the JNK inhibitor SP600125 (1 μm), for 36 hours Apoptosis was then assessed by DNA fragmentation assay. RANKL-mediated apoptosis was abrogated by the JNK inhibitor in *Rela*^{-/-} cells. The data are representative of 3 independent experiments. [†]P < 0.05 *Rela*^{-/-} versus *Rela*^{+/+} or *Rela*^{-/-} with SP600125. (**D**) *Rela*^{+/+} and *Rela*^{-/-} BMMs were cultured in osteoclastogenic conditions for 8 days, with or without SP600125 for the first 36 hours, showing rescue of differentiation with short-term JNK inhibition. Scale bar: 200 μm.

transduced with retroviral siRNA hairpins were decreased 85% for siBid1 and 55% for siBid2 compared with those transduced with an irrelevant siRNA-targeting luciferase, siLuc (Figure 5B). Culture of the same set of BMMs in RANKL showed a reduction of apoptosis back to *Rela*^{+/+} levels (Figure 5C) and restored OC numbers after 6 days of culture (Figure 5D). Furthermore, analysis of bone resorption by OCs derived from siBid-transduced BMMs demonstrated that the function of surviving OCs was intact (Figure 5, E and F). The degree of Bid knockdown correlated with rescue of apoptosis, differentiation, and function. Thus, RelA opposes a proapoptotic pathway mediated by JNK and Bid in OC precursors.

Protection from RANKL-induced apoptosis is specific for RelA and not RelB. Previous studies of the function of NF-κB in OCs, including our own study of NIK (8, 9), have not established unique roles for individual subunits. Therefore, we examined the effect of RelA on the κB DNA-binding activity of RelB, controlled by the alternative

NF-κB pathway, and c-Rel, controlled by the classical NF-κB pathway. In RANKL-stimulated BMMs, levels of RelB κB-binding activity are similar in the presence and absence of RelA (Figure 6A), indicating that activation of the alternative pathway is not affected in these mice. The κB DNA-binding activity of c-Rel is also unchanged in *Rela*^{-/-} cultures compared with *Rela*^{+/+} cultures, suggesting that c-Rel does not perform the same function as RelA.

To further address whether the classical subunit RelA has a distinct function from the alternative NF-κB subunit RelB, we analyzed apoptosis in RelB-deficient cultures. In contrast to *Rela*^{-/-} BMMs, *Relb*^{-/-} BMMs did not undergo apoptosis when cultured for 48 hours in the presence of RANKL (Figure 6B). Next, we asked if the overexpression of RelB could rescue the apoptosis induced by RANKL in RelA-deficient OC precursors by using retroviral vectors to transduce *Rela*^{-/-} BMMs. Immunoblots confirmed retroviral-mediated expression of both subunits (Figure 6C). As expected, expression of RelA reduced

Figure 5
Knockdown of Bid rescues *Rela*−/− osteoclastogenesis. (**A**) *Rela*+/+ and *Rela*−/− BMMs were stimulated with RANKL at the indicated times, and total cell lysates were examined by immunoblot for expression of Bid. β-actin was used as loading control. (**B**) *Rela*−/− BMMs were transduced with retrovirus expressing 2 different siRNAs for Bid (siBid1 and siBid2) or luciferase (siLuc). Following puromycin selection, levels of Bid were examined by immunoblot, demonstrating reduction of Bid by the specific siRNAs. β-actin was used as loading control. (**C**) *Rela*+/+ and *Rela*−/− BMMs transduced with siLuc or siBid1 or -2 were cultured with RANKL for 36 hours and DNA fragmentation was measured. The data are representative of 3 independent experiments. *$P < 0.05$ versus *Rela*+/+ siLuc. (**D**) The same BMMs in **C** were cultured in osteoclastogenic conditions for 6 days, then stained for TRAP, showing rescue of differentiation with knockdown of Bid. Scale bar: 200 μm. (**E**) BMMs cultured on cortical bone slices were stained with horseradish peroxidase-conjugated wheat germ agglutinin to demonstrate resorption. Scale bar: 200 μm. (**F**) Pits in **E** were quantified, showing that reduction in apoptosis correlates with differentiation and bone resorption. Black bars indicate *Rela*+/+; gray bars indicate *Rela*−/−; *$P < 0.05$ versus *Rela*+/+ siLuc.

apoptosis to *Rela*+/+ levels (Figure 6D) and fully restored osteoclastogenesis in *Rela*−/− cells (Figure 6E). In contrast, retroviral expression of RelB did not affect levels of apoptosis and did not rescue osteoclastogenesis in *Rela*−/− BMMs, despite the ability of this construct to rescue the RelB-deficient phenotype (21). Thus, we conclude that the subunit RelA specifically protects OC precursors from RANKL-induced apoptosis, and RelB cannot compensate for its absence.

Discussion

Many studies have demonstrated that NF-κB is an important therapeutic target in inflammatory diseases, including arthritis. However, it is also clear that NF-κB is critical for many normal cel-

lular functions and that global inhibition over prolonged periods, such as would be required in the treatment of chronic diseases, is likely to cause unacceptable side effects. Therefore, determining more restricted NF-κB targets is an important goal. The NF-κB family has 5 members, and although each subunit has been genetically ablated in mice, few subunit-specific roles have been defined in the context of disease models. In this study, we have focused on the prototypical subunit RelA/p65 and have delineated its role in the OC in vivo and in vitro.

The key cytokine for OC differentiation is RANKL, a member of the TNF superfamily. Like TNF-α, RANKL potently activates the classical NF-κB pathway with rapid nuclear translocation and
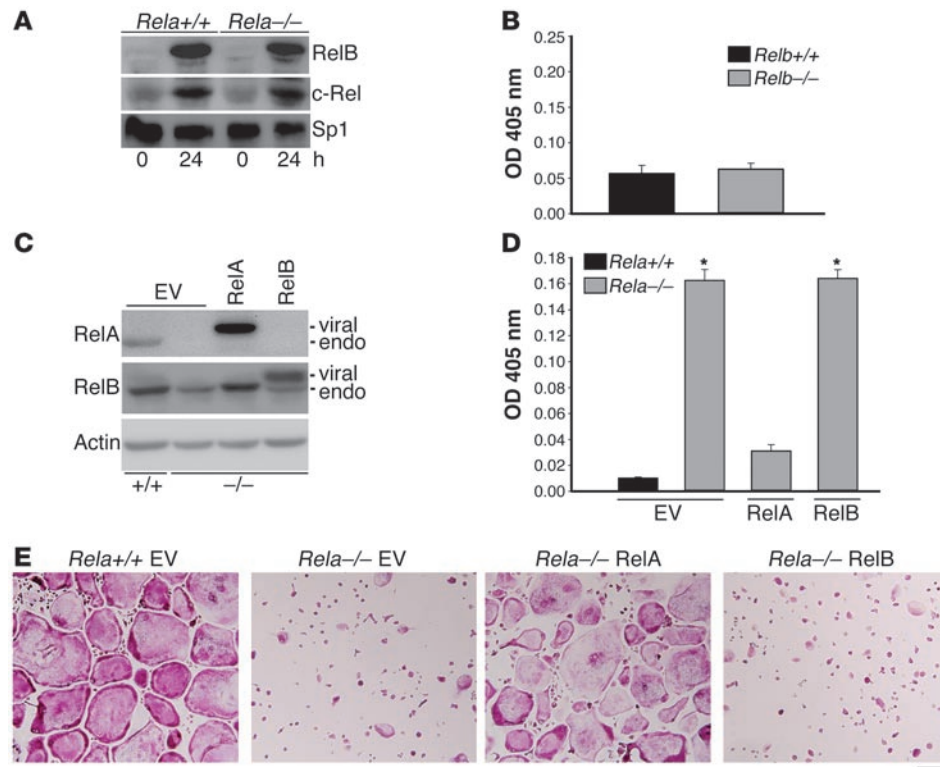
Figure 6
Enhanced RANKL-induced apoptosis is specific for *RelA*. (**A**) BMMs from *Rela*$^{+/+}$ and *Rela*$^{-/-}$ mice were cultured in the presence of M-CSF and RANKL for 0 or 24 hours. Equal amounts of nuclear extracts were incubated with biotinylated κB oligos bound to streptavidin-coated beads. Beads were washed to isolate κB-bound proteins, and these were analyzed by immunoblot for RelB or c-Rel. Unbound nuclear proteins were analyzed by immunoblot for Sp1 as loading control. (**B**) BMMs from *Relb*$^{+/+}$ and *Relb*$^{-/-}$ mice were cultured with M-CSF and RANKL for 48 hours, and apoptosis was assessed by DNA fragmentation assay, showing no effect of RelB on apoptosis. (**C**) *Rela*$^{-/-}$ BMMs retrovirally transduced with empty vector (EV), RelA, or RelB, and *Rela*$^{+/+}$ BMMs transduced with EV were selected in blastocydin, then analyzed by immunoblot. Viral-encoded proteins (both RelA and RelB), migrate more slowly than their endogenous (endo) counterparts, and are expressed at 2- to 3-fold over endogenous levels. (**D**) BMMs transduced in **C** were cultured with RANKL for 48 hours, and apoptosis was assessed by DNA fragmentation assay. While the EV control and RelB vectors do not abrogate the RANKL-induced cell death in *Rela*$^{-/-}$ cultures, RelA reduces apoptosis to the same level as *Rela*$^{+/+}$ transduced with EV. *$P < 0.001$ *Rela*$^{+/+}$ EV. (**E**) Transduced BMMs were grown in osteoclastogenic conditions for 6 days and then were fixed and stained for TRAP. Reexpression of RelA restores *Rela*$^{-/-}$ OC differentiation, while overexpression of RelB has no effect. Scale bar: 200 μm.

trast to TNFR1, RANK does not have a death domain, and therefore, lacks an obvious mechanism by which to induce apoptosis. Nevertheless, at least 1 study using the RAW cell line (13) has suggested that RANKL can induce apoptosis in OC precursors dependent on JNK but independent of classical NF-κB. We find that in primary marrow macrophages lacking both RelA and TNFR1, RANKL is a potent inducer of apoptosis mediated by JNK, Bid, and caspase-3. The effect is dependent on the loss of RelA and not TNFR1, since the phenotype is not changed by reexpression of TNFR1. Furthermore, Li et al. (22) recently examined the bone phenotype of TNFR1-deficient mice and found elevated bone formation, due to increased osteoblast activity, but no change in bone resorption or OC parameters. These data support our conclusion that RANKL alone is able to induce apoptosis in OC precursors in the absence RelA, independent of TNF effects. Additionally, because TNF can cause apoptosis via TNFR1 in RelA-deficient cells (23), we would predict that the absence of TNFR1 would be more likely to reduce the apoptotic response (as occurs in hepatocytes), rather than potentiate it.

The mechanism by which JNK activation leads to cell death has only been studied in the context of TNF signaling. Franzoso and colleagues (18, 24) have shown that RelA mediates transcription of Gadd45β, an inhibitor of MKK7, the activating kinase for JNK. In their model, absence of RelA downregulates Gadd45β, leading to prolonged activation of MKK7 and JNK in response to TNF. This aberrantly activated JNK causes cleavage of the proapoptotic Bcl-2 family member Bid to an active jBid form, leading to its translocation to the mitochondria and activation of the caspase-3 pathway (25). We find that RANKL fails to upregulate Gadd45β, as well as MKP5, in the absence of RelA and that activation of JNK is enhanced. Short-term blockade of JNK activation prevents RANKL-induced apoptosis in OC precursors, allowing their differentiation, as does reduction of Bid levels by siRNA. However, we are unable to detect the appearance of cleaved forms of Bid in our *Rela*$^{-/-}$ OC precursors, suggesting that there may be some differences in the pathways due to the cell lineage or the receptor initiating the pathway. In the context of anoikis (cell death induced by lack of adhesion), Bid can be activated without cleavage (26).

In the TNF pathway, ROS have been identified as the key mediator of the crosstalk between the NF-κB and JNK (27). In situations of impaired NF-κB signaling, generation of ROS is required for

DNA binding of RelA-containing dimers. Blockade of this classical pathway, by mutation or inhibition of IKKβ or IκB-superrepressors, prevents activation of RelA and blocks osteoclastogenesis (5, 7, 14). It therefore appeared that RelA was an important mediator of OC differentiation. We found that although *Rela*$^{-/-}$ precursors do not differentiate well in standard osteoclastogenic culture conditions, this effect is completely dependent on an increase in apoptosis. When cell death is blocked, differentiation proceeds and fully functional bone-resorbing OCs are generated. We therefore conclude that RelA is not specifically required for the OC differentiation transcriptional program.

TNFR1 bears a death domain in its cytoplasmic tail and can cause apoptosis via caspase-8. The role of NF-κB in opposing this apoptotic TNF pathway has been studied extensively in several systems, and transcriptional targets have been described. In the OC lineage, blockade of classical NF-κB leads to TNF-mediated apoptosis (5, 6). In con-

TNF-mediated apoptosis. In the OC lineage, however, inhibition of ROS reduces differentiation and bone resorption (28, 29). JNK activation is also required for OC differentiation (30–32). RANKL activates both ROS and JNK, and these linked pathways contribute both differentiation and apoptotic signals. In the presence of RelA, apoptosis is suppressed and generation of OCs is optimal, while in the absence of RelA, precursor apoptosis reduces the number of mature bone-resorbing cells. Thus, there is a tight range of JNK activation required for osteoclastogenesis, and RelA is a critical component in maintaining appropriate levels. Furthermore, inhibition of caspases or JNK within the first 2 days of RANKL culture restores differentiation in $Rela^{-/-}$ OC precursors, suggesting that timing of JNK activation might be as important as the magnitude.

Karin and coauthors (33) showed that TNF-α–mediated JNK activation induces apoptosis by accelerating turnover of the NF-κB regulated protein c-FLIP, an inhibitor of caspase-8, by upregulating the E3 ubiquitin ligase Itch. However, in $Rela^{-/-}$ OC precursors RANKL does not induce caspase-8 activation, so it is unlikely that c-FLIP and Itch are important mediators in response to RANKL.

RelA and RelB appear to have distinct functions in the OC lineage. In the absence of RelA, OC precursors readily undergo apoptosis in response to RANKL but are capable of full differentiation and function if cell death is blocked. In contrast, RelB-deficient precursors are not susceptible to RANKL-mediated apoptosis but have a defect in differentiation (21). Absence of RelA does not affect signaling by RelB, and overexpression of the latter does not rescue the apoptotic $Rela^{-/-}$ phenotype. Another major difference between RelA and RelB is the kinetics of their activation by RANKL. RelA is activated within minutes of exposure of BMMs to RANKL and is relatively transient, while RelB activation takes hours and persists for days (D.V. Novack, unpublished observations). Whether the differences in RelA and RelB function lie in their upstream control mechanisms (IKKβ and NIK, respectively) or in the structure of the subunits themselves remains to be determined.

Previous studies have shown that inhibition of the classical NF-κB pathway blocks both inflammation and bone erosion in several models of inflammatory arthritis. We have now used radiation chimeras bearing bone marrow from $Rela^{-/-}Tnfr1^{-/-}$ mice or from $Rela^{+/+}Tnfr1^{-/-}$ controls in the serum transfer model of arthritis. Despite the fact that hematopoietic cells in these RCs are unable to respond directly to TNF, inflammation develops with or without RelA. However, the presence of RelA was critical for the OC response. The number of OCs adjacent to inflammatory pannus on bone surfaces and their activity as measured by serum CTX levels were both markedly blunted in $Rela^{-/-}$ RCs. This effect is most likely mediated by RANKL, as opposed to other cytokines present during arthritis, since $Rela^{-/-}$ RCs also have a poor osteoclastogenic response to injection of exogenous RANKL.

In summary, we have demonstrated that despite the absence of a cytoplasmic death domain, RANK activates a proapoptotic pathway similar to that induced by TNFR1, with JNK, Bid, and caspase-3 playing key roles. The NF-κB subunit RelA has a central, subunit-specific function in blocking this cell death to allow differentiation but is not required for the transcription of genes required for osteoclastogenesis.

Methods

Mice. $Rela^{-/-}Tnfr1^{-/-}$ and $relb^{-/-}$ mice were maintained by heterozygote matings in a specific pathogen-free facility. The genotype of all mice used was confirmed by PCR analysis of genomic DNA extracted from tail biopsies.

All experimental protocols were approved by the Institutional Animal Studies Committee at Washington University School of Medicine.

Bone marrow transplantation. Recipient 3- to 5-week-old C57BL/6J mice (The Jackson Laboratory) were administered 10 Gy total-body γ-irradiation 1 day prior to injection of 1×10^6 bone marrow cells from $Rela^{+/+}Tnfr1^{-/-}$ or $Rela^{-/-}Tnfr1^{-/-}$ donors via tail vein. The engraftment of transplanted marrow was confirmed by western blot for RelA (data not shown) on BMMs from the RCs.

Serum transfer arthritis. Arthritis was induced by intraperitoneal injection of 250 μl K/BxN serum at days 0, 2, and 7, with 50 μg LPS (*E. coli* 011; B4; Sigma-Aldrich) on day 2 as described (9). Ankle thickness in the hind paws was measured by dial gauge (Mitutoyo).

In vivo RANKL treatment. $Rela^{+/+}$ and $Rela^{-/-}$ RCs were injected subcutaneously with GST-RANKL (500 μg per day for 5 days) or PBS (sham).

Measurement of serum TRAP5b and CTX. Immediately prior to sacrifice, mice were anesthetized and bled retro-orbitally. After clotting and centrifugation, serum was collected and stored at –80°C prior to analysis using Mouse TRAP assay (IDS Inc.) or CTX (Rat Lap Elisa; Nordic Bioscience Diagnostic) according to the manufacturer's instructions.

Bone histomorphometry. Mouse lumbar vertebrae, calvariae, or ankle joints were fixed overnight in formalin and decalcified in 14% EDTA. Paraffin-embedded sections were stained with H&E or for TRAP activity. Bone sections were coded prior to analysis. Trabecular bone volume (BV/TV), OC surface (Oc.S/BS.), and OC numbers (N.Oc./B.Pm.) were measured by an observer blinded to genotype according to a standard protocol using Bioquant Osteo (Bioquant Image Analysis Corporation).

OC culture. BMMs were obtained and differentiated into OCs as described (34), using CMG14-12 as a source of M-CSF and recombinant GST-RANKL. For osteoclastogenesis in 96-well plates, BMMs from $Rela^{-/-}$ and $Rela^{+/+}$ mice were plated at 5×10^3 and cultured with 30 ng/ml of M-CSF (1:50 CMG supernatant). After 5 to 6 days the wells were fixed with 4% paraformaldehyde and OCs were visualized by histochemical staining for TRAP activity according to manufacturer's instructions (Sigma-Aldrich). For coculture experiments, calvarial OCs and BMMs from $Rela^{-/-}$ and $Rela^{+/+}$ mice were mixed at a ratio of 1:2 and cultured for 7 days in the presence of 1,25 vitamin D$_3$ (10^{-8} M) (Sigma-Aldrich).

Bone pit staining. BMMs were differentiated on bovine cortical bone slices with RANKL for 7–8 days. The staining of resorption lacuna was performed as described previously (35). Briefly, the cells were removed from the bone slices by wiping the surface of the bone slices with a soft brush, then slices were rinsed, incubated with 20 μg/ml peroxidase-conjugated wheat germ agglutinin (Sigma-Aldrich) for 30 minutes, and developed with 3, 3'-diaminobenzidine for 15 minutes.

MTT assay. BMMs were cultured in M-CSF, with or without GST-RANKL, for 3 to 48 hours, and the number of viable cells was measured by adding 10 μl MTT 5 mg/ml (3-4, 5-dimethylthiazol-2y-2,5 diphenyltetrazolium bromide; Sigma-Aldrich) to 200 μl culture medium in each well and incubated at 37°C for 4 hours. To stop the reaction, 150 μl 0.04 N HCl in isopropanol was added to each well, and absorbance was determined at 570 nm.

DNA fragmentation assay. Cell death detection assay was performed with the Cell Death Detection Elisa kit (Roche Diagnostics Corp.) according to manufacturer's instructions. $Rela^{+/+}$ and $Rela^{-/-}$ BMMs were cultured in 96-well plates for 36–48 hours in the presence of M-CSF (1:50 CMG supernatant) and GST-RANKL (150 ng/ml), with or without 10 μM ZVAD-FMK (R&D Systems) or the JNK inhibitor, SP600125 (1.0 μM) (Calbiochem) prior to lysis. Absorbance was read at 405 nm using Bio-Rad Microplate Reader.

Caspase activation fluorometric assays. The activation of caspase-3, -8, or -9 was measured according to the protocol of their respective fluorometric kits (Biovision). Cells in suspension were collected by centrifugation and mixed with adherent cells for lysis. Substrates were DEVD-AFC (cas-

pase-3), FLICE (caspase-8), and LEHD-AFC (caspase-9). Fluorescence was read using Spectra Fluor (Tecan) with 400-nm excitation filter and 505-nm emission filter.

Retroviral transduction. Retrovirus was generated by cloning murine relA (with an N-terminal HA tag) or relB cDNAs into the pMX-IRES-bsr vector adapted for the Gateway cloning system (Invitrogen) and transfected into platE packaging cells, using Transfectol (Gene Choice). Replication incompetent viral supernatant was added to BMMs for 24 hours, along with 4 μg/ml polybrene (Sigma-Aldrich), prior to selection with blastocydin (1 μg/ml) for 3 days. Surviving, transduced BMMs were then cultured in a similar fashion to primary, unmanipulated BMMs. siRNAs for Bid were designed using the Dharmacon website (http://www.dharmacon.com/DesignCenter) and cloned as a small hairpin into pSuper retroviral vector bearing the U6 promoter. SiBid1 sequence derived from the 3′ untranslated region is 5′-CAGCTTGAGTGTATCTGAA-3′; SiBid2 sequence derived from the open reading frame is 5′-GCTCTGGCTGTACTCGCCA-3′. PlatE packaging cells were transfected and BMMs were transduced as for the PMX vectors but with puromycin (2 μg/ml) selection, and the expression levels for BID were analyzed by western blot.

Immunoblotting analysis. Total protein was extracted as described (8). The proteins were quantitated with DC protein assay kit (Bio-Rad), and 40–50 μg of total protein were resolved by SDS-polyacrilamide gel electrophoresis under reducing conditions and then transferred to PVDF membrane. The blots were incubated for 1 hour in 5% dry milk and subsequently, overnight with the specific antibodies for pJNK, total JNK (Cell Signalling); RelA, RelB, c-Rel, SP1, β-actin (Santa Cruz Biotechnology Inc.); or Bid (R&D Systems); followed by anti-rabbit or anti-mouse HRP-conjugated secondary antibodies (Santa Cruz Biotechnology Inc.). Blots were evaluated by chemiluminescence using SuperSignal substrates (Pierce) and imaged with Genesnap, using the Syngene Imaging System (Synoptics). Relative protein expression was determined using Genetools (Synoptics).

κB pulldown assay. Nuclear extract (30 μg) was incubated with streptavidin-coated agarose beads preincubated with biotinylated κB3 oligonucleotide (8) for 30 minutes at 4°C on a rotator in 1x binding buffer (30 mM NaCl, 10 mM Tris, pH 7.4, 1 mM EDTA, 5% glycerol, 1 mg/ml BSA, and 1 mM DTT) with 1 μg poly dIdC. Beads were then washed in 1x binding buffer 3 times prior to SDS-PAGE and immunoblotted for RelB and/or c-Rel.

Real-time PCR. Total RNA was extracted using RNeasy (QIAGEN), and cDNA was generated with AMV-RT (Fisher) according to manufacturers' instructions using 1 μg total RNA and oligo-dT primers diluted to a final volume of 100 μl. Quantitative RT-PCR was performed on an ABI7300 Real-Time PCR system (Applied Biosystems) using SYBR Green PCR Master Mix assay (Applied Biosystems). The standard curve used a series of duplicate dilutions of plasmid for each gene and GAPDH cDNA. The amplification reaction was performed for 40 cycles with denaturation at 95°C for 10 minutes, followed by annealing at 95°C for 15 seconds, and extension and detection at 60°C for 1 minutes. The relative RNA abundance of each target gene transcript was normalized against endogenous gene control and calculated as $2^{-\Delta ct}$ (target gene – endogenous control gene), where ct represents the threshold cycle for each transcript.

Primers are as follows: *Gapdh*, 5′-CTTCACCACCATGGAGAAGGC-3′ and 5′-GACGGACACATTGGGGGGTAG-3′; *Xiap*, 5′-TGCAAGAGCTG-GATTTTATGC-3′ and 5′-GGTCTTCACTTGGCTTCCAAT-3′; *Gadd45b*, 5′-TACGAGGCGGCCAAACTGATGAAT-3′ and 5′-ACGACTGGAT-CAGGGTGAAGTGAA-3′; *Mkp5*, 5′-GAGAAAGGCCTCTTCAACTACAA-3′ and 5′-CCACACTGGTGAGCTTCCTC-3′.

Statistics. Data are presented as mean ± SEM. Statistical significance was determined by 2-tailed Student's t test using SigmaPlot (SSPS). P values ≤ 0.05 were considered significant.

Address correspondence to: Deborah Veis Novack, Washington University School of Medicine, 660 S. Euclid Ave., Box 8301, St. Louis, Missouri 63110, USA. Phone: (314) 454-8472; Fax: (314) 454-5047; E-mail: novack@wustl.edu.

1. Teitelbaum, S.L. 2007. Osteoclasts: what do they do and how do they do it? *Am. J. Pathol.* **170**:427–435.
2. Perkins, N.D. 2007. Integrating cell-signalling pathways with NF-κB and IKK function. *Nat. Rev. Mol. Cell Biol.* **8**:49–62.
3. Franzoso, G., et al. 1997. Requirement for NF-κB in osteoclast and B-cell development. *Genes Dev.* **11**:3482–3496.
4. Iotsova, V., et al. 1997. Osteopetrosis in mice lacking NF-κB1 and NF-κB2. *Nat. Med.* **3**:1285–1289.
5. Ruocco, M.G., et al. 2005. IκB kinase (IKK)β, but not IKKα, is a critical mediator of osteoclast survival and is required for inflammation-induced bone loss. *J. Exp. Med.* **201**:1677–1687.
6. Abbas, S., and Abu-Amer, Y. 2003. Dominant-negative IκB facilitates apoptosis of osteoclasts by tumor necrosis factor-α. *J. Biol. Chem.* **278**:20077–20082.
7. Abu-Amer, Y., Dowdy, S.F., Ross, F.P., Clohisy, J.C., and Teitelbaum, S.L. 2001. TAT fusion proteins containing tyrosine 42-deleted IκBα arrest osteoclastogenesis. *J. Biol. Chem.* **276**:30499–30503.
8. Novack, D.V., et al. 2003. The IκB function of NF-κB2 p100 controls stimulated osteoclastogenesis. *J. Exp. Med.* **198**:771–781.
9. Aya, K., et al. 2005. NF-κB–inducing kinase controls lymphocyte and osteoclast activities in inflammatory arthritis. *J. Clin. Invest.* **115**:1848–1854.
10. Beg, A.A., Sha, W.C., Bronson, R.T., Ghosh, S., and Baltimore, D. 1995. Embryonic lethality and liver degeneration in mice lacking the RelA component of NF-kappa B. *Nature.* **376**:167–170.
11. Beg, A.A., and Baltimore, D. 1996. An essential role for NF-kappaB in preventing TNF-alpha-induced cell death. *Science.* **274**:782–784.
12. Van Antwerp, D.J., Martin, S.J., Kafri, T., Green, D.R., and Verma, I.M. 1996. Suppression of TNF-α-induced apoptosis by NF-κB. *Science.* **274**:787–789.
13. Bharti, A.C., Takada, Y., Shishodia, S., and Aggarwal, B.B. 2004. Evidence that receptor activator of nuclear factor (NF)-κB ligand can suppress cell proliferation and induce apoptosis through activation of a NF-κB-independent and TRAF6-dependent mechanism. *J. Biol. Chem.* **279**:6065–6076.
14. Jimi, E., et al. 2004. Selective inhibition of NF-κB blocks osteoclastogenesis and prevents inflammatory bone destruction in vivo. *Nat. Med.* **10**:617–624.
15. Clohisy, J.C., et al. 2003. Direct inhibition of NF-κB blocks bone erosion associated with inflammatory arthritis. *J. Immunol.* **171**:5547–5553.
16. Korganow, A., et al. 1999. From systemic T cell self-reactivity to organ-specific autoimmune disease via immunoglobulins. *Immunity.* **10**:451–461.
17. Salvesen, G.S., and Duckett, C.S. 2002. IAP proteins: blocking the road to death's door. *Nat. Rev. Mol. Cell Biol.* **3**:401–410.
18. De Smaele, E., et al. 2001. Induction of gadd45β by NF-κB downregulates pro-apoptotic JNK signalling. *Nature.* **414**:308–313.
19. Kamata, H., et al. 2005. Reactive oxygen species promote TNFalpha-induced death and sustained JNK activation by inhibiting MAP kinase phosphatases. *Cell.* **120**:649–661.
20. Papa, S., Zazzeroni, F., Pham, C.G., Bubici, C., and Franzoso, G. 2004. Linking JNK signaling to NF-κB: a key to survival. *J. Cell Sci.* **117**:5197–5208.
21. Vaira, S., et al. 2008. RelB is the NF-κB subunit downstream of NIK responsible for osteoclast differentiation. *Proc. Natl. Acad. Sci. U. S. A.* **105**:3897–3902.
22. Li, Y., et al. 2007. Endogenous TNFα lowers maximum peak bone mass and inhibits osteoblastic Smad activation through NF-κB. *J. Bone Miner. Res.* **22**:646–655.
23. Ruocco, M.G., et al. 2005. IκB kinase (IKK)β, but not IKKα, is a critical mediator of osteoclast survival and is required for inflammation-induced bone loss. *J. Exp. Med.* **201**:1677–1687.
24. Papa, S., et al. 2007. Insights into the structural basis of the GADD45beta-mediated inactivation of the JNK kinase, MKK7/JNKK2. *J. Biol. Chem.* **282**:19029–19041.
25. Deng, Y., Ren, X., Yang, L., Lin, Y., and Wu, X. 2003.

A JNK-dependent pathway is required for TNFα-induced apoptosis. *Cell.* **115**:61–70.

26. Valentijn, A.J., and Gilmore, A.P. 2004. Translocation of full-length Bid to mitochondria during anoikis. *J. Biol. Chem.* **279**:32848–32857.

27. Papa, S., et al. 2006. The NF-κB-mediated control of the JNK cascade in the antagonism of programmed cell death in health and disease. *Cell Death Differ.* **13**:712–729.

28. Lee, N.K., et al. 2005. A crucial role for reactive oxygen species in RANKL-induced osteoclast differentiation. *Blood.* **106**:852–859.

29. Kim, H.J., et al. 2006. Antioxidant α-lipoic acid inhibits osteoclast differentiation by reducing nuclear factor-κB DNA binding and prevents in vivo bone resorption induced by receptor activator of nuclear factor-κB ligand and tumor necrosis factor-α. *Free Radic. Biol. Med.* **40**:1483–1493.

30. Yamanaka, Y., Abu-Amer, Y., Faccio, R., and Clohisy, J.C. 2006. Map kinase c-JUN N-terminal kinase mediates PMMA induction of osteoclasts. *J. Orthop. Res.* **24**:1349–1357.

31. David, J.-P., Sabapathy, K., Hoffmann, O., Idarraga, M.H., and Wagner, E.F. 2002. JNK1 modulates osteoclastogenesis through both c-Jun phosphorylation-dependent and -independent mechanisms. *J. Cell Sci.* **115**:4317–4325.

32. Lee, S.K., Gardner, A.E., Kalinowski, J.F., Jastrzebski, S.L., and Lorenzo, J.A. 2006. RANKL-stimulated osteoclast-like cell formation in vitro is partially dependent on endogenous interleukin-1 production. *Bone.* **38**:678–685.

33. Chang, L., et al. 2006. The E3 ubiquitin ligase itch couples JNK activation to TNFalpha-induced cell death by inducing c-FLIP(L) turnover. *Cell.* **124**:601–613.

34. Faccio, R., Novack, D.V., Zallone, A., Ross, F.P., and Teitelbaum, S.L. 2003. Dynamic changes in the osteoclast cytoskeleton in response to growth factors and cell attachment are controlled by β3 integrin. *J. Cell Biol.* **162**:499–509.

35. Zhao, H., Laitala-Leinonen, T., Parikka, V., and Vaananen, H.K. 2001. Downregulation of small GTPase Rab7 impairs osteoclast polarization and bone resorption. *J. Biol. Chem.* **276**:39295–39302.